09.2;09.3

Mechanism of suprawavelength microstructures formation on metal surfaces by linear polarized ultrashort laser radiation

© V.S. Makin[1,2], R.S. Makin[3]

[1] Branch of the „Kometa“ Corporation for Special Purpose Space Systems — Scientific and Design Center for Optoelectronic Observation Complexes, St. Petersburg, Russia
[2] Peter the Great St. Petersburg Polytechnic University — Institute of Nuclear Power Engineering, Sosnovyi Bor, Leningrad Oblast, Russia
[3] National Research Nuclear University „MEPhI“, Moscow, Russia
E-mail: vladimir.s.makin@gmail.com

Received July 3, 2023
Revised September 18, 2023
Accepted September 19, 2023

The model for suprawavelength structures formation based on the experimental data of nano- and microrelief of metal surface evolution under linear polarized laser radiation and on the nonlinear mathematical model of ordered spatial periods formation was suggested. The model is based taking into account the mutual interference of surface plasmon polaritons propagating in neighbouring directions and is applicable for oxidizing metals.

Keywords: metal, surface plasmon-polariton, universal polariton model, surface morphology, nano-/micrograting, oxide film.

DOI: 10.61011/TPL.2023.11.57194.19673

The model of formation of subwavelength resonance periodic structures on metal surfaces by ultrashort pulsed laser radiation (LR) has been proposed for the first time and verified experimentally in [1]. A considerable number of studies reporting the observations of formation of interrelated suprawavelength nano- and micrograting structures (in what follows, they are referred to simply as structures) on metal and semiconductor surfaces under the influence of ultrashort pulsed LR have been published in the last decade. However, an explanation for the formation of suprawavelength structures has been formulated only in the case of their normal orientation ($\mathbf{g} \parallel \mathbf{E}$) [2]; no mechanism of formation of anomalously oriented ($\mathbf{G} \perp \mathbf{E}$) structures has been proposed [3–7]. Here, $\mathbf{E}$ is the LR electric field vector; lowercase and uppercase letters $\mathbf{g}$ and $\mathbf{G}$ denote grating (structure) vectors corresponding to normal and anomalous orientations. Experimental studies into the formation of so-called thermochemical laser-induced periodic surface structures (TLIPSSs) of an anomalous orientation have been published in recent years. It proved difficult to determine the mechanism of their formation [7]. A model based on LR scattering by metal surface irregularities into TE surface plasmon polaritons (SPPs) [8] (under the assumption that $\mathbf{G}$ is an interference grating formed with a contribution from TE SPPs) has been proposed. In the present study, a model of formation of suprawavelength structures of an anomalous orientation ($\mathbf{G}$) with consideration of the mutual interference of SPPs, where these structures are regarded as one of the possible stages of evolution of the resonance nanorelief morphology ($\tilde{\mathbf{g}}$) driven by the mutual interference of SPPs propagating in neighboring directions, is proposed. Here, $\tilde{\mathbf{g}}$ is a superposition of resonance gratings with a certain spread of directions around the primary one, which is specified by vector $\mathbf{E}$, and equal periods.

Let us examine the model more closely. Gratings $\tilde{\mathbf{g}}$ with their depth h increasing with number of pulses N form under the influence of linearly polarized radiation (normal incidence). At h on the order of several tens of nanometers, the efficiency of dissipation of converted LR into SPPs becomes equal to the absorption capacity of the metal surface. The mutual interference of SPPs needs to be taken into account in this case [9]. The directions of most efficient SPP excitation become isolated (from angular spectrum $\Delta\varphi$ of SPP propagation directions; see Fig. 1) in a self-organizing nonlinear dissipative dynamic LR−metal system. Aided by their spatial overlapping and interference, this results in the formation of large-scale gratings $\tilde{\mathbf{G}}$ (with spatial scale $\tilde{D} \geqslant \lambda$, where λ is the LR wavelength), which are nearly orthogonal to $\mathbf{E}$ [9]. Structures $\tilde{\mathbf{G}}$ differ from gratings $\mathbf{g}$ in having a greater spread of periods and directions. However, if LR scanning at rate $\mathbf{v}$ is implemented, selection of SPP excitation directions is effected (in particular, at $\mathbf{v} \parallel \mathbf{E}$), structures $\tilde{\mathbf{g}}$ gradually become oriented (see, e.g., [10,11]), and a grating orthogonal to direction $\mathbf{E}$, $\mathbf{G} \perp \mathbf{E}$, forms: two orthogonal gratings $\mathbf{g}$ and $\mathbf{G}$ overlap. Experiments have demonstrated that the growth of the control value (energy density Q or number N of pulses) leads to an abrupt variation of period $\tilde{D}$ (see, e.g., the experimental data for brass in Fig. 2 [12]). This change is triggered by two factors: first, angular spectrum $\Delta\varphi$ becomes narrower as N (or Q) increases; second, the periods of gratings $\mathbf{g}$ are discrete and increase with Q [13]. Their enhancement translates into a discrete growth of $\tilde{D}$ (see Table 1, which is based on the data from Fig. 2; f is the spatial frequency

Table 1. Period d of microstructures of a normal orientation ($\mathbf{g}$) and characteristic spatial scale $\tilde{D}$ of structures of an anomalous orientation ($\tilde{\mathbf{G}}$) formed on brass at a fixed number of pulses $N_{eff} = 1600$ and various energy densities Q of ultrashort pulsed LR ($\lambda = 800\,\text{nm}$, $\tau = 125\,\text{fs}$). The data from Fig. 2 were used to determine these values (grating vectors and periods are denoted by lowercase and uppercase letters in the case of normal ($\mathbf{g} \parallel \mathbf{E}$) and anomalous orientations, respectively)

Q, J/cm^2	d_{exp}, μm	d_{theor}, λ/η	η	$\tilde{D}_{exp}$, μm	$\tilde{D}_{theor}$, λ/ξ	ξ
0.36	0.6; 1.2	3/4; 3/2	~ 1	1.36	2	1.18
0.45	0.6; 1.2	3/4; 3/2	~ 1	1.5	2	1.07
0.52	0.6; 1.2	3/4; 3/2	~ 1	1.66	2	~ 1
0.60	0.6; 1.2	3/4; 3/2	~ 1	1.66	2	~ 1
0.68	0.6; 1.6	3/4; 2	1.0; 1.0	3.16	4	1.02
0.82	2.8	4	1.14	6.31	8	1.02
1.06	2.8	4	1.14	7.1	9	1.01

Note. Two structure periods, which form in the same irradiation region (and are normally spaced apart within the region) at a given Q value, are indicated for d_{exp} and d_{theor} . Grating data from [12] (Fig. 8) are provided in the end row of the table.

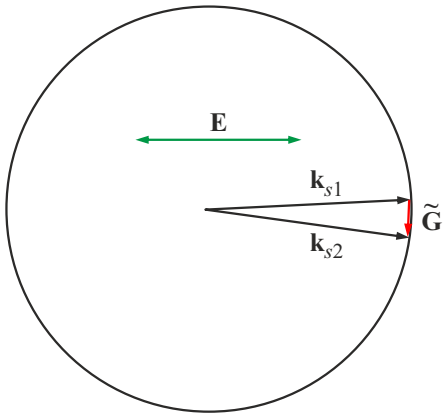

Figure 1. Circle vector diagram illustrating the momentum conservation law and the mutual interference of surface plasmon polaritons having wave vectors $\mathbf{k}_{s1}$, $\mathbf{k}_{s2}$, which propagate in neighboring directions, with the formation of suprawavelength grating $\tilde{\mathbf{G}}$ that is nearly orthogonal to vector $\mathbf{E}$.

of structures). Discrete values of theoretical period d_{theor} of grating $\mathbf{g}$ were determined with the use of a nonlinear mathematical model (NMM) of formation of spatial periods of structures within the framework of the universal polariton model (UPM) of laser-induced destruction of condensed media [2,14] and agree with experimental data [15,16]. The following notation is used in Table 1: η is the real part of the complex refraction index of the air–brass interface for SPPs; ξ characterizes the difference between theoretical period $\tilde{D}_{theor}$ and experimental period $\tilde{D}_{exp}$ of grating $\tilde{\mathbf{G}}$ and is a quantity comparable to η; and d_{exp} is the experimental value of the period of grating $\mathbf{g}$. It can be seen from Table 1 that the growth of $\tilde{D}_{exp}$ is correlated with the growth of experimental period d_{exp} of grating $\mathbf{g}$ and starts at $Q = 0.68\,\text{mJ/cm}^2$. The evolution of periods of gratings $\mathbf{g}$ governs the formation of gratings $\tilde{\mathbf{G}}$ upon their spatial overlapping and shapes the resultant surface morphology (Figs. 1 and 2).

The geometric treatment of vectors $\mathbf{k}_{s1}$, $\mathbf{k}_{s2}$, and $\tilde{\mathbf{G}}$ (Fig. 1) and experimental angular spread $\Delta\varphi$ of SPP propagation directions provide a theoretical estimate of the spatial scale of grating $\tilde{\mathbf{G}}$: $\tilde{D}_{theor} = (2-3)k\lambda$, where $k = d_{theor}\eta/\lambda$ is taken from the third column of Table 1. Thus, the coupling between the characteristics of normal and anomalous gratings was estimated. This estimate clarifies the experimental discrete growth of $\tilde{D}$ in steps of λ. As was demonstrated earlier [2,14,17], variations of d_{exp} follow the Sharkovskii ordering [18,19], and variations of $\tilde{D}$ governed by this quantity also follow the same ordering, which is typical of such nonlinear dynamic systems (see, e.g., [2,14]).

The transformations of relief on brass are associated with the mechanism of „recording“ of structures in a melting–crystallization cycle. If metals are processed in an oxidizing atmosphere, relief $\tilde{\mathbf{G}}$ may be „recorded“ by modulating the thickness of an oxide film (at low values of Q), which hinders strongly the transformation of relief [13,20–26]. Let us examine the specifics of this regime using the example of ultrashort pulsed LR ($\lambda = 1026\,\text{nm}$, $\tau = 232\,\text{fs}$, $\nu = 200\,\text{kHz}$, $v = 3.5\,\mu\text{m/s}$, and the spot diameter is $14.7\,\mu\text{m}$) incident on chromium films in air at low scanning rates ($v \leqslant 10\,\mu\text{m/s}$) [20]. Gratings $\mathbf{g}$ ($d_{theor} = \lambda/3\eta \approx 300-400\,\text{nm}$) were observed first, and structures $\tilde{\mathbf{G}}$ formed after that (Fig. 3). Following the same procedure of $\tilde{D}$ estimation that was used for brass, we find $\tilde{D} \leqslant \lambda \approx 1026\,\text{nm}$, which correlates with the experimental data: $\tilde{D}_{exp} \approx 930\,\text{nm}$ (Table 2).

According to our model, the properties of structures $\tilde{\mathbf{G}}$ differ substantially from the properties of resonance structures type $\mathbf{g}$ (i.e., the so-called periodic surface structures, PSSs) [27], since (1) the orientation of structures $\tilde{\mathbf{G}}$ may differ significantly from perpendicular $\mathbf{E}$ (by up to 20–30°) and have a wide directional spread (this remains true in the $\mathbf{v} \perp \mathbf{E}$ geometry), which was observed experimentally [8,20]; (2) the experimentally observed spread for $\tilde{D}$ is substantially more pronounced compared to d_{exp} for PSSs (especially at $\mathbf{v} \perp \mathbf{E}$) [24]; (3) structures $\tilde{\mathbf{G}}$ are secondary in relation to $\mathbf{g}$; (4) the mechanism of their „recording“ is

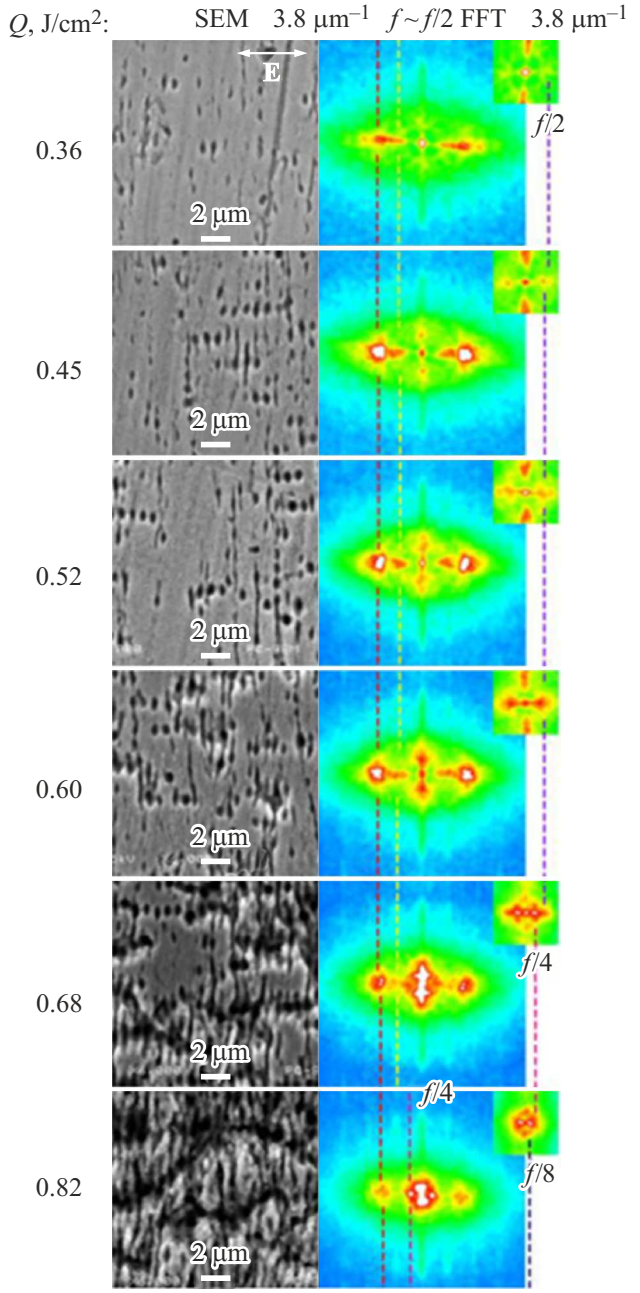

Figure 2. Left column: magnified images of regions of a polished brass surface irradiated with a series of linearly polarized laser radiation ($\lambda = 800$ nm, $\tau = 125$ fs) pulses ($N_{eff} = 1600$). These images were obtained with a scanning electron microscope (SEM). Right column: the corresponding fast Fourier transforms of the surface relief at various energy densities of laser radiation Q, which are indicated in the left part of the image. Spatial frequencies f of gratings are converted into periods in accordance with the following relation: $f/k \to k\lambda$ [12].

modulation of an oxide film thickness; (5) structures $\tilde{\mathbf{G}}$ scale with the LR wavelength [23] (usually as $\sim\lambda$; see Table 2); (6) in experiments with the air pressure increasing from $2.2 \cdot 10^{-5}$ Pa, a smooth transition from the formation of gratings with $\mathbf{g} \parallel \mathbf{E}$ ($d = \lambda/2\eta \approx 338$ nm) and gratings

Table 2. Characteristic spatial scales $\tilde{D}_{exp}$ of gratings $\tilde{\mathbf{G}}$ formed on the surface of a titanium film with a thickness of 90 nm under the influence of laser radiation with different wavelengths and with LR scanning in direction $\mathbf{v} \parallel \mathbf{E}$ [23]

Parameter		λ, nm		
		1026	513	256
$\tilde{D}_{exp}$, nm	Vacuum	943 ± 30	416 ± 17	182 ± 22
	Air	853 ± 20		
	Nitrogen, 2.5 atm	940 ± 23		
Q, mJ/cm²		70	50	35
v, μm/s		1	3	1

$\mathbf{G} \perp \mathbf{E}$ ($d = \lambda/4\xi \approx 172$ nm) on titanium, where gratings $\mathbf{G}$ modulate the ridges of grating $\mathbf{g}$, to PSSs ($d = \lambda/2\eta$) and structures $\tilde{\mathbf{G}} = (\tilde{D}_{exp} \approx 0.6\,\mu\text{m} \approx \tilde{D}_{theor} \approx 0.67\,\mu\text{m}$ at $2 \cdot 10^3$ Pa) was observed [25]. Here, ξ is the real part of the refraction index of the metal–air interface for wedge SPPs propagating along waveguiding protruding relief elements of PSSs with a transverse subwavelength spatial scale [28]. The mentioned experimental features, which are uncharacteristic of PSSs, provide support for our theory that explains the formation of structures $\tilde{\mathbf{G}}$ (TLIPSSs) on oxidizing metals in numerous experiments [13,20–26]. Thus, the model characterizes well the results of numerous experiments with metals [3,7,29], oxidizing metals [13,20–26], semiconductors [5], and, possibly, dielectrics [30].

We note in conclusion that an NNM- and UPM-based model of formation of suprawavelength microstructures of an anomalous orientation was proposed. The model relies on mutual interference of SPPs propagating in neighboring directions that are excited by linearly polarized LR pulses on metal surfaces. The dynamic interdependent coexistence and development of spatially overlapping gratings $\mathbf{g}$ and suprawavelength surface structures of an anomalous orientation was noted. It was demonstrated that the spatial scale of suprawavelength structures varies discretely and proportionally to the LR wavelength in accordance with the Sharkovskii ordering. The model is also applicable to semiconductors and is consistent with a large set of experimental data. It characterizes well the formation of TLIPSSs if one takes into account the distinct nature of relief „recording“ in the form of modulation of thickness of an oxide film that hinders strongly the transformation of anomalous structures. The model is consistent with numerous experiments into structuring of surfaces of oxidizing metals and into the dynamics of surface morphology. It is universal in the sense of applicability to metals, semiconductors, and, possibly, dielectrics. The obtained results may be used in the field of laser processing of materials with substantially different physical properties.

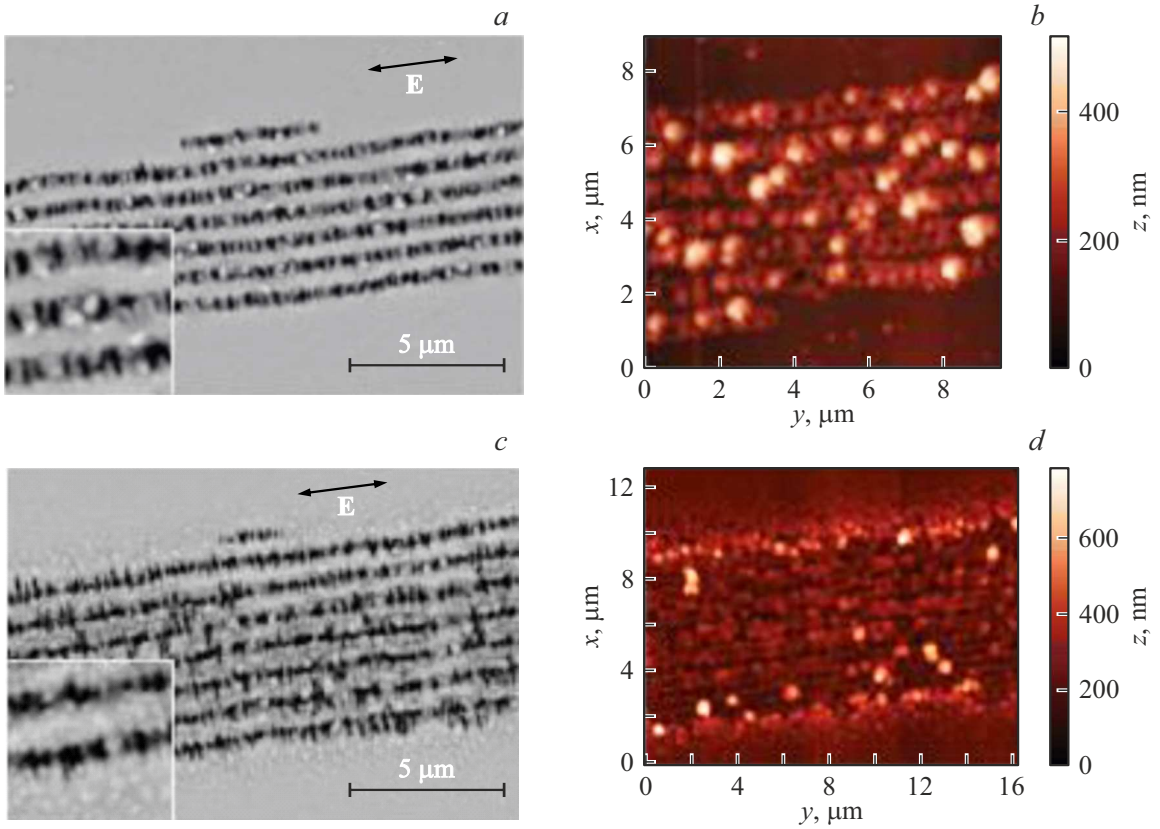

Figure 3. SEM images of TLIPSSs formed on the surface of a chromium film by laser radiation with energy $E = 83$ (*a*) and 10^2 nJ (*c*) and the corresponding images obtained with an atomic force microscope (*b*, *d*). Magnified images of overlapping structures $\mathbf{g} + \tilde{\mathbf{G}}$ [20] are shown in the insets (panels *a* and *c*).

Conflict of interest

The authors declare that they have no conflict of interest.

References

[1] M.B. Agranat, S.I. Ashitkov, V.E. Fortov, S.I. Anisimov, A.M. Dykhne, P.S. Kondratenko, JETP, **88** (2), 370 (1999). DOI: 10.1134/1.558805.

[2] V.S. Makin, R.S. Makin, A.Ya. Vorob'ev, Ch. Guo, in *Nelineinost' v sovremennom estestvoznanii*, Ed. by G.G. Malinetskii (LKI, M., 2009), pp. 302–322 (in Russian).

[3] J. Bonse, S. Höhm, S. Kirner, A. Rosenfeld, J. Krüger, IEEE J. Sel. Top. Quantum Electron., **23** (3), 9000615 (2017). DOI: 10.1109/JSTQE.2016.2614183

[4] J. Bonse, Nanomaterials, **10** (10), 1950 (2020). DOI: 10.3390/nano10101950

[5] J.J.J. Nivas, S. Amoruso, Nanomaterials, **11** (1), 174 (2021). DOI: 10.3390/nano11010174

[6] D. Zhang, R. Liu, Z. Li, Int. J. Extrem. Manuf., **4** (1), 015102 (2022). DOI: 10.1088/2631-7990/ac376c

[7] K.M.T. Ahmmed, C. Grambow, A.-M. Kietzig, Micromachines, **5** (4), 1219 (2014). DOI: 10.3390/mi5041219

[8] A.V. Dostovalov, T.J.Y. Derrien, S.A. Lizunov, F. Přeučil, K.A. Okotrub, T. Mocek, V.P. Korolkov, S.A. Babin, N.M. Bulgakova, Appl. Surf. Sci., **491**, 650 (2019). DOI: 10.1016/j.apsusc.2019.05.171

[9] V.V. Bazhenov, A.M. Bonch-Bruevich, M.N. Libenson, V.S. Makin, Pis'ma Zh. Tekh. Fiz., **10** (24), 1520 (1984) (in Russian).

[10] S. Durbach, N. Hampp, Appl. Phys. Lett., **121** (25), 251601 (2022). DOI: 10.1063/5.0128227

[11] V.N. Anisimov, V.Yu. Baranov, L.A. Bol'shov, A.M. Dykhne, D.D. Malyuta, V.D. Pis'mennyi, A.Yu. Sebrant, M.A. Stepanova, Poverkhn.: Fiz., Khim., Mekh., No. 7, 138 (1983) (in Russian).

[12] M. Huang, F. Zhao, Y. Cheng, N. Xu, Z. Xu, Opt. Express, **18** (S4), A600 (2010). DOI: 10.1364/OE.18.00A600

[13] B. Öktem, I. Pavlov, S. Ilday, H. Kalaycioğlu, A. Rybak, S. Yavaş, M. Erdoğan, F.Ö. Ilday, Nat. Photon., **7**, 897 (2013). DOI: 10.1038/nphoton.2013.272

[14] V.S. Makin, R.S. Makin, A.Ya. Vorobyev, C. Guo, Tech. Phys. Lett., **34** (5), 387 (2008). DOI: 10.1134/S1063785008050088.

[15] J.M. Preston, H.M. van Driel, J.E. Sipe, Phys. Rev. B, **40** (6), 3942 (1989). DOI: 10.1103/PhysRevB.40.3942

[16] O.P. Gashkov, M.N. Libenson, V.S. Makin, V.V. Trubaev, Pis'ma Zh. Tekh. Fiz., **18** (10), 32 (1992) (in Russian).

[17] V.S. Makin, R.S. Makin, Opt. Spectrosc., **112** (2), 162 (2012). DOI: 10.1134/S0030400X12020208.

[18] A.N. Sharkovskii, Ukr. Mat. Zh., **16** (1), 61 (1964) (in Russian); A.N. Sharkovskii, Ukr. Mat. Zh., **17** (3), 104 (1965) (in Russian).

[19] T. Li, J.A. Yorke, Am. Math. Monthly, **82** (10), 985 (1975). http://links.jstor.org/sici?sici=0002-9890%28197512%2982%3A10%3C985%3APTIC%3E2.0.CO%3B2-H
[20] A.V. Dostovalov, V.P. Korolkov, V.S. Terentyev, K.A. Okotrub, F.N. Dultsev, S.A. Babin, Quantum Electron., **47** (7), 631 (2017). DOI: 10.1070/QEL16379.
[21] D.A. Belousov, K.A. Bronnikov, K.A. Okotrub, S.L. Mikerin, V.P. Korolkov, V.S. Terentyev, A.V. Dostovalov, Materials, **14** (21), 6714 (2021). DOI: 10.3390/ma14216714
[22] Y.C. Guan, W. Zhou, Z.L. Li, H.Y. Zheng, G.C. Lim, M.H. Hong, Appl. Phys. A, **115** (1), 13 (2014). DOI: 10.1007/s00339-013-7927-5
[23] A.V. Dostovalov, V.P. Korolkov, S.A. Babin, Laser Phys. Lett., **12** (3), 036101 (2015). DOI: 10.1088/1612-2011/12/3/036101
[24] K. Bronnikov, S. Gladkikh, K. Okotrub, A. Simanchuk, A. Zhizhchenko, A. Kuchmizhak, A. Dostovalov, Nanomaterials, **12** (3), 306 (2022). DOI: 10.3390/nano12030306
[25] H. Xie, B. Zhao, Y. Lei, Z. Yu, J. Cheng, J. Yang, Opt. Express, **29** (20), 31408 (2021). DOI: 10.1364/OE.433035
[26] K.A. Bronnikov, S.A. Gladkikh, K.A. Okotrub, V.P. Korol'kov, A.A. Kuchmizhak, A.V. Dostovalov, Kvantovaya Elektron., **52** (11), 1012 (2022) (in Russian).
[27] V.S. Makin, R.S. Makin, *Osnovy vzaimodeistviya ul'trakorotkogo lazernogo izlucheniya s kondensirovannymi sredami* (Dimitrovgrad, 2013) (in Russian).
[28] V.S. Makin, E.I. Logacheva, R.S. Makin, Opt. Spectrosc., **120** (4), 610 (2016). DOI: 10.1134/S0030400X16040172.
[29] M. Tsukamoto, T. Kayahara, H. Nakano, M. Hashida, M. Katto, M. Fujita, M. Tanaka, N. Abe, J. Phys.: Conf. Ser., **59**, 666 (2007). DOI: 10.1088/1742-6596/59/1/140
[30] G.D. Tsibidis, E. Skoulas, A. Papadopoulos, E. Stratakis, Phys. Rev. B, **94** (8), 081305(R) (2016). DOI: 10.1103/PhysRevB.94.081305

Translated by D.Safin